

Fundamental parameters of Galactic luminous OB stars

V. The effect of microturbulence*

M.R. Villamariz¹ and A. Herrero^{1,2}

¹ Instituto de Astrofísica de Canarias, E-38200 La Laguna, Tenerife, Spain

² Departamento de Astrofísica, Universidad de La Laguna, Avda. Astrofísico Francisco Sánchez, s/n, E-38071 La Laguna, Spain

15 December 1999 / 14 March 2000

Abstract. We study the effect of microturbulence in the line formation calculations of H and He lines, in the parameter range typical for O and early B stars. We are specially interested in its effect on the determination of stellar parameters: T_{eff} , $\log g$ and specially on the He abundance.

We first analyze the behaviour of H and He model lines between 4000 and 5000 Å with microturbulence and find that for O stars only He I lines and He II λ 4686 are sensibly affected by microturbulence, and that models with lower gravities, the ones suitable for supergiants, are more sensitive to it.

Using a test procedure we show that the expected changes in T_{eff} , $\log g$ and Helium abundance due to the inclusion of microturbulence in the analysis, are small. We analyze five stars (two late, one intermediate and two early O stars) using microturbulence velocities of 0 and 15 kms^{-1} and confirm the result of the previous test. The parameters obtained for 15 kms^{-1} differ from the ones at 0 kms^{-1} within the limits of the standard error box of our analysis. Only later types reduce their He abundance, by 0.02 in ϵ . Comparing with values in the literature we find that the range of our changes agree with previous results. In some cases other effects can add to microturbulence, and further reduce the He abundance up to 0.04. The quality of the line fits only improves for He I λ 4471, but not to the extent of completely solving the so-called dilution effect.

Therefore our conclusion is that microturbulence is affecting the derivation of stellar parameters, but its effect is comparable to the adopted uncertainties. Thus it can reduce moderate He overabundances and solve line fit quality differences, but it cannot explain by itself large He overabundances in O stars.

Key words: Stars: atmospheres – Stars: early-type – Stars: fundamental parameters – Line: formation – Line: profiles – Turbulence

1. Introduction

Although microturbulence is a fundamental parameter when deriving abundances from stellar spectra, it has been systematically ignored when deriving He abundances from quantitative spectroscopical NLTE analyses of OB stars (Herrero et al. 1992, Smith & Howarth 1994), being the first exceptions to this the works by McErlean et al. (1998) and Smith & Howarth (1998).

One of the main reasons to ignore it is that the use of NLTE techniques reduced the need of microturbulence for the reproduction of the observed metallic line strengths and they even made abundances less sensitive to the value adopted for microturbulence than in LTE analyses (Becker & Butler 1989).

In quantitative NLTE analyses of OB stars, the lines of H and He are used to determine stellar parameters (namely, effective temperature, T_{eff} , logarithmic surface gravity, $\log g$, and He abundance). Their line profiles are dominated by the Stark broadening, and microturbulence, included in the standard way, only adds an extra Doppler width to the thermal broadening. First values for microturbulence found in LTE for main sequence B stars, of the order of 5 kms^{-1} (Hardorp & Scholz 1970), showed to be small enough to be of no importance when compared to H and He thermal velocities, that in such hot atmospheres are well above 5 kms^{-1} . This together with the use of NLTE made the influence of microturbulence in the overall profile seem negligible.

When measuring microturbulence in OB supergiants the situation is quite different, as its value has always showed to be comparable or well above the thermal velocities of H and He, and even, in some cases, above the speed of sound in these atmospheres (Lamers 1972, Lennon & Dufton 1986). This was not changed by later NLTE analyses (Lennon et al. 1991, Hubeny et al. 1991, Gies & Lam-

Send offprint requests to: M.R. Villamariz

* The INT is operated on the island of La Palma by the RGO in the Spanish Observatorio de El Roque de los Muchachos of the Instituto de Astrofísica de Canarias.

Correspondence to: ccid@ll.iac.es

bert 1992, Smartt et al. 1997), in which the values of microturbulence obtained are usually reduced but never to values clearly without contradiction. Kudritzki (1992) and Lamers & Achmad (1994) explained that this could be due to the presence of wind outflow in these stars, that can mimic the effect of microturbulence in the line profiles.

Most of the previously referred works are on early B and late O supergiants. Little work has been done on early O stars (see Hubeny et al. 1991), mainly because for them, with scarce metallic lines, it is very difficult to measure the value of microturbulence. And it is in the whole range of O stars that we are interested.

One problem that is systematically found in all analyses of OB spectra is the impossibility of finding a consistent fit of all He I lines with a unique set of parameters. This difficulty appears worse in supergiants than in main sequence stars, and it is bigger between results from singlet and from triplet lines, but also appears within different lines in one system. We call this the He I *lines problem*.

This discrepancy between singlet and triplet lines of He I was investigated by Voels et al. (1989), who considered that atmospheric extension was responsible and so they called this effect “generalized dilution effect”. But recent works with spherical, mass losing models show that this can not be the only reason (Herrero et al., 1995, 2000). Furthermore, McErlean et al. (1998) and Smith & Howarth (1998) find that the inclusion of microturbulence in the line formation calculations reduces, although not to all its extent, the discrepancy between the fits of singlet and triplet lines. They also find better and more consistent fits for the whole set of He I lines when microturbulence is considered.

One more reason that encourages us to study the effect of microturbulence is that a careful inspection of several works shows that even for main sequence stars, values of microturbulence comparable to the thermal velocities of at least He are obtained in NLTE (Gies & Lambert 1992, Kilian et al. 1991), which can invalidate the hypothesis of negligible influence of microturbulence in the profiles.

So in this paper we want to study microturbulence in the range of parameters typical for O stars of any luminosity class, specifically pointing to its effect on the determination of stellar parameters and also on the He I *lines problem*. We are specially interested in investigating whether the inclusion of microturbulence can solve the *He discrepancy* (Herrero et al. 1992), as Vrancken (1997), McErlean et al. (1998) and Smith & Howarth (1998) suggest. This now well known problem has induced a lot of theoretical improvements in both evolutionary and model atmosphere theories in order to explain it. Recent works including sphericity and mass loss in the spectral analysis (Herrero et al. 1995, 2000, Israelian et al. 2000) show that with these new models, more suitable for these stars than the plane-parallel hydrostatic ones, the discrepancy is not solved. Evolutionary models including additional mixing inside the star can explain enhanced He photospheric

abundances during the H-burning phase, this mixing being induced by different physical mechanisms like rotation and turbulent diffusion (Dennisenkov, 1994, Meynet & Maeder, 1997, Maeder & Zahn, 1998), or turbulent diffusion and semiconvection (Langer 1992). Sometimes angular rotational velocity changes during evolution are included (Langer & Heger, 1998, Heger, 1998). For a recent review, see Maeder & Meynet (2000). Therefore it becomes of great importance to see whether microturbulence can be responsible for the *He discrepancy*.

In Sect. 2 we present line formation calculations of H and He lines and their behaviour with microturbulence in the O stars domain. In Sect. 3 we determine the effect of including microturbulence in the determination of stellar parameters, and in Sect. 4 we analyze some stars with and without considering microturbulence. Sections 5 and 6 are then dedicated to our discussion and conclusions, respectively .

2. Microturbulence in H and He line formation calculations

In order to study the behaviour of H and He lines with microturbulence, we perform line formation calculations in the parameter range typical for O to early B stars of any luminosity class:

- between 30 000 and 45 000 K in T_{eff}
- between 3.05 and 4.00 in $\log g$ (in c.g.s. units)
- for $\epsilon = 0.10$ and 0.20 , with $\epsilon = \frac{N(\text{He})}{N(\text{He})+N(\text{H})}$

where $N(x)$ is the number density of atom X. We follow the classical technique of calculating a NLTE model atmosphere of H and He, in radiative and hydrostatic equilibrium and with plane-parallel geometry (calculated with ALI, see Kunze, 1995), and then solve the statistical equilibrium and transfer equations and perform the formal solution for the lines of H and He chosen using DETAIL & SURFACE (Butler & Giddings 1985). In this final step we have included UV metal line opacities in the calculations, in order to obtain more realistic profiles (see Herrero, 1994, and Herrero et al., 2000, for details). As shown in the last reference, plane-parallel models are unable to reproduce properly spectra of massive OB stars around 50 000 K and hotter, that is why we stop our study at 45 000K.

Microturbulence is introduced in the standard way, by adding an extra Doppler width to the thermal broadening of the line, which is then convolved with the rest of the broadening mechanisms. We have considered it in both the equations of statistical equilibrium and radiative transfer. As we don’t consider other motions (turbulent or not) in the determination of the stellar structure, we prefer to restrict the introduction of microturbulence to the absorption coefficient. Therefore, we do not include it in the calculation of the structure of the atmosphere via turbulent pressure. For similar reasons also we do not even bother about its dependence on depth. We don’t treat separately the effect on the populations and line profiles, as this has

been recently studied by McErlean et al. (1998) and Smith & Howarth (1998) (whose results we support).

We make line formation calculations for the lines we usually consider to perform our analyses: H_γ and H_β for $H\text{ I}$; $\text{He I } \lambda\lambda 4387, 4922, 4471 \text{ \AA}$ for He I ; and $\text{He II } \lambda\lambda 4200, 4541, 4686 \text{ \AA}$ for He II .

In order to study the behaviour of these lines with microturbulence, we perform line formation calculations for microturbulence velocity values from 0 to 20 km s^{-1} , for different sets of parameters, representing the spectral types and luminosity classes we are interested in:

– $T_{\text{eff}} = 30\,000$, $\log g = 3.05$, $\epsilon = 0.10$ for late O and early B supergiants. The same with $\log g = 4.00$ for dwarfs.

– $T_{\text{eff}} = 35\,000$, $\log g = 3.20$, $\epsilon = 0.10$ for “middle” O supergiants. The same with $\log g = 4.00$ for dwarfs.

– $T_{\text{eff}} = 40\,000$, $\log g = 3.40$, $\epsilon = 0.10$ for early O supergiants. The same with $\log g = 4.00$ for dwarfs.

– $T_{\text{eff}} = 45\,000$, $\log g = 3.60$, $\epsilon = 0.10$ for very early O supergiants. The same with $\log g = 4.00$ for dwarfs.

The values of $\log g$ for supergiants are close to the lowest that could be converged for every T_{eff} . For dwarfs of increasing T_{eff} , $\log g$ becomes a little below 4.00, but this value still represents well this luminosity class. Finally, these calculations were repeated for $\epsilon = 0.20$, to look for differential effects with He abundance.

Figs. 1, 2 and 3 display the behaviour of H and He line profiles with microturbulence, for three different models, adequate respectively for late O supergiants, late O dwarfs and early O supergiants. In Table 1 equivalent widths are given for all these lines. The first two Figs. will allow us to compare the effects of microturbulence when varying $\log g$, whereas the first and last Figs. will be used to compare the effects when varying T_{eff} . The other calculated models behave consistently with what it is shown in Figs. 1–3 and will not be further discussed.

Looking first at Fig. 1 we see that there are two different line groups. The first one is composed by the strong H lines and the relatively weak lines $\text{He II } \lambda\lambda 4200, 4541$. All these lines are not affected by microturbulence, although our highest values are comparable to the thermal velocity of H atoms and well above that of He atoms. The reason is that the Stark broadening dominates the profiles, and therefore masks the changes that microturbulence produce.

The second group is composed by He I lines and the strong He II $\lambda 4686$ line. He I lines show sensitivity to microturbulence in both core and wings, while the core of He II $\lambda 4686$ is desaturated by microturbulence, but its effect is masked in the wings by the Stark broadening, because, as it has been explained by Smith & Howarth (1998), the effect of microturbulence will depend on the steepness of the line wings.

When we then compare Figs. 1 and 2 we see that the increased pressure broadening (directly related to the increased density) simply reduces the effect of microturbulence in the line profiles. Thus, as gravity increases, the

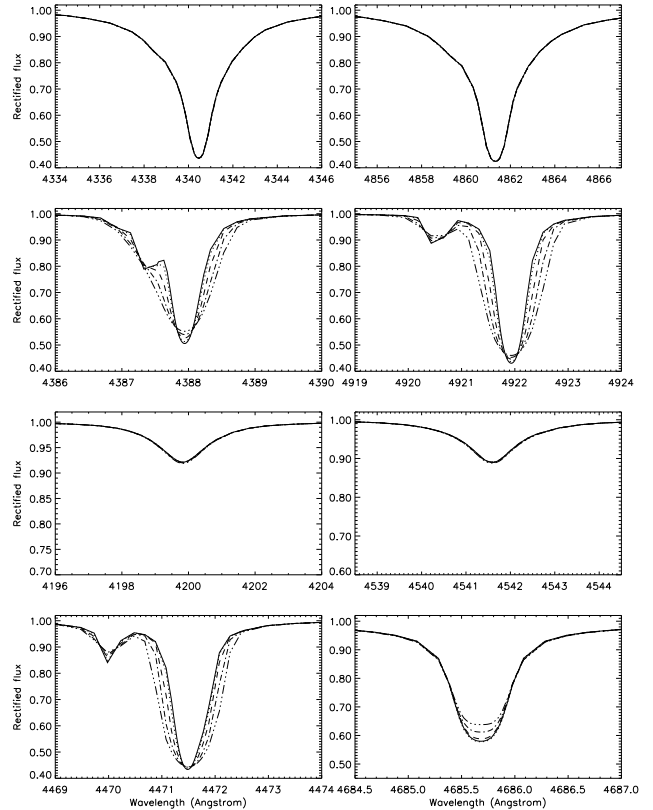


Fig. 1. From top to bottom and left to right: H_γ , H_β , $\text{He I } \lambda\lambda 4387, 4922$, $\text{He II } \lambda\lambda 4200, 4541$, $\text{He I } \lambda 4471$, $\text{He II } \lambda 4686$, for the model with $T_{\text{eff}} = 30\,000$, $\log g = 3.05$, $\epsilon = 0.10$, representing late O and early B supergiants. Microturbulence takes values of 0 (solid line), 5 (dotted), 10 (dashed), 15 (dash dotted) and 20 (dash tri-dotted) km s^{-1} .

effect of microturbulence decreases for all considered lines. In the case of He II lines this effect is reinforced by the displacement introduced in the He ionization equilibrium, that makes He II lines weaker.

More interesting is the comparison with higher temperatures. Looking to Fig. 1 and Fig. 3 we can see the behaviour of the lines of supergiants with increasing T_{eff} . For higher values of T_{eff} marginal effects on H I and He II line cores are seen (Fig. 3), but only He I lines and He II $\lambda 4686$ are again really sensitive to microturbulence. He II line profiles are still insensitive, although they are now much stronger and even have a larger equivalent width than He I lines, because they are dominated by the Stark broadening. The reason why He I line profiles are still sensitive to microturbulence, although they are much weaker, has to be found in the influence of microturbulence on the shape of the absorption profile of weak lines. Thus, we see that He I $\lambda\lambda 4387, 4922$ are not saturated in the whole temperature range. Their equivalent widths increase with increasing microturbulence, until, as T_{eff} increases, they become weak enough to have equivalent widths, but not line profiles, independent of microturbulence. This hap-

Table 1. Equivalent widths of the lines in Figs. 1, 2 and 3, in mÅ. For every line the values for microturbulence velocities of 0, 5, 10, 15 and 20 kms⁻¹ are given from top to bottom. Model parameters in the first column are T_{eff} in K, $\log g$ in cgs units and ϵ .

Params.	H γ	H β	He I 4387	He I 4922	He I 4471	He II 4200	He II 4541	He II 4686
30 000	1895	2149	403	503	622	195	234	416
3.05	1896	2150	415	526	637	195	234	418
0.10	1896	2151	446	585	682	196	235	415
	1904	2160	485	664	750	199	238	410
	1904	2173	525	753	836	201	241	401
30 000	3831	3832	599	733	1158	42	50	161
4.00	3832	3833	605	747	1167	42	50	160
0.10	3834	3836	618	780	1189	42	50	157
	3839	3843	636	825	1220	42	50	151
	3850	3857	654	873	1252	42	50	145
40 000	2005	2393	120	238	391	491	614	685
3.40	2004	2392	118	240	402	491	613	684
0.10	2001	2385	118	255	434	492	613	685
	2020	2406	120	279	480	519	646	667
	2011	2392	120	299	530	522	649	669

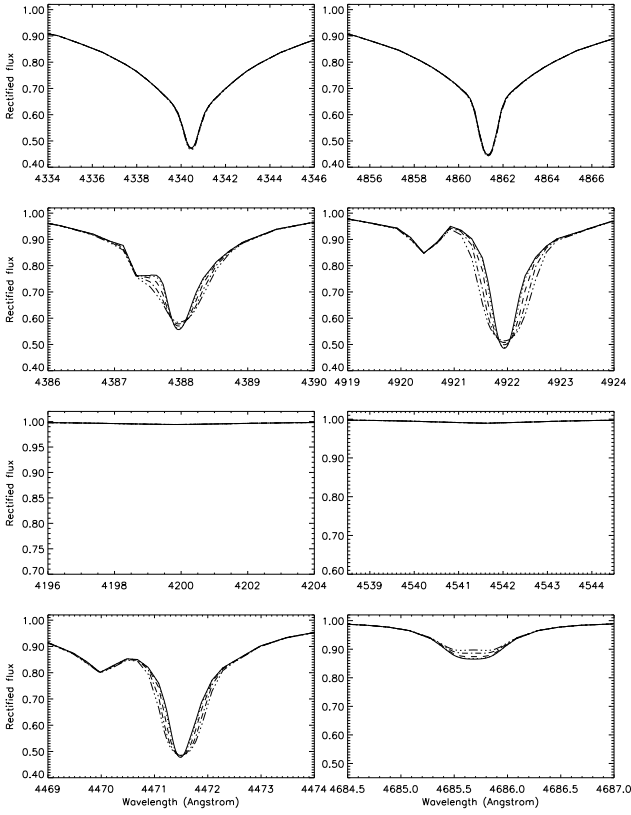


Fig. 2. Same as Fig. 1, but for $\log g = 4.00$, representing late O and early B dwarfs.

pens at 40 000 K for He I λ 4387 (see Table 1) and at 45 000 K for He I λ 4922. For them, Doppler broadening is important enough to let microturbulence shape the profiles appreciably in the whole temperature range. He I λ 4471 is saturated at $T_{\text{eff}} = 30\,000$ K, but it desaturates at $T_{\text{eff}} = 35\,000$, and starts behaving like the other He I lines.

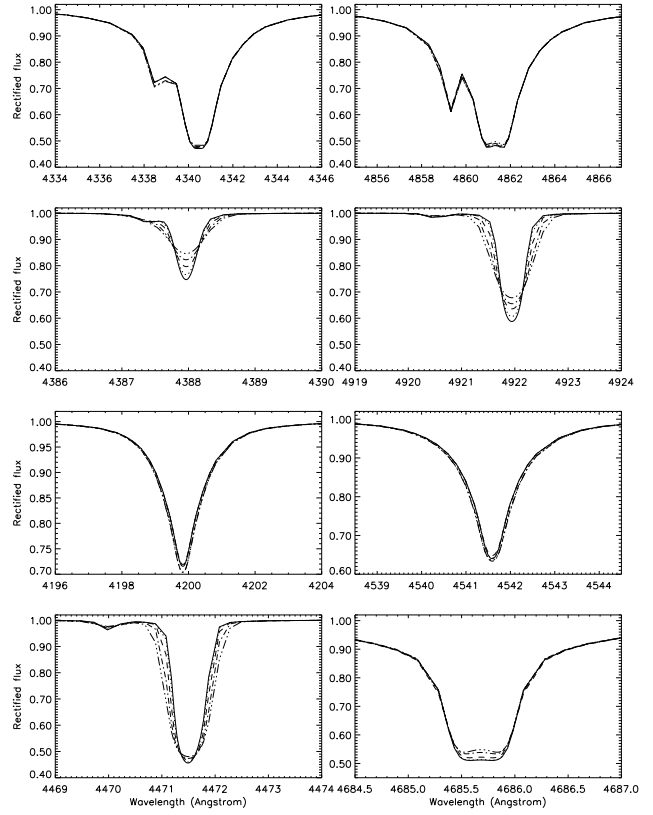


Fig. 3. Same as Fig. 1, but for $T_{\text{eff}} = 40\,000$, $\log g = 3.40$, $\epsilon = 0.10$, representing early O supergiants

Finally, we point out that all these results also apply for models with $\epsilon = 0.20$, and that they are a natural extension to O stars of the results of Mc Erlean et al. (1998) and Smith & Howarth (1998).

3. The influence of microturbulence in the determination of parameters of O-stars

In this work we are interested in estimating the changes introduced in the derived stellar parameters by the inclusion of microturbulence in the analysis of O stars, with special attention to its influence in the derived He abundance. As we saw in the previous section, models of low gravity, corresponding to supergiants, are more sensitive to microturbulence, and so we expect supergiants to show the largest changes.

Values of microturbulence of 10, 12 kms^{-1} are found for late O and early B stars (see references in the introduction), therefore we decided to choose a fixed value for microturbulence of 15 kms^{-1} to perform a test of the influence of microturbulence in the determination of T_{eff} , $\log g$ and He abundance.

As a first approach to the problem, we take a model spectrum at $\xi=15 \text{ kms}^{-1}$ as the *observed* spectrum, to which we fit model profiles in a grid around it at $\xi=0 \text{ kms}^{-1}$, with parameters differing in 500 to 1000 K in T_{eff} , 0.05 to 0.10 in $\log g$ and 0.02 to 0.04 in ϵ (these small values are suggested by previous inspection of a larger, coarser grid). To maximize the effect of microturbulence, we consider neither rotational broadening nor instrumental broadening. Taking advantage of the fact that we are using only theoretical profiles (although the one with $\xi=15 \text{ kms}^{-1}$ has been adopted as *the observation*) we use a least-squares fit procedure to determine the best fit.

For each line of each model in the grid, we calculate the quadratic difference with the *observed* line, and then we add the results for all lines of a given ion. For example for H we calculate:

$$\chi_i^2(\text{H}) = \sum_{H \text{ lines}} \frac{1}{\Delta\lambda} \sum_{\lambda} w_{\lambda} (f_{\lambda, \text{grid}} - f_{\lambda, \text{obs}})^2$$

as the result for H for model i of the grid, where w_{λ} is the spectral sampling and $\Delta\lambda$ is the wavelength interval containing the whole line. We perform these calculations for all the models in the grid and then normalize these values to their minimum, so that a 1.00 gives us the model that best fits the lines of the ion at all temperatures, gravities and He abundances. The calculation is performed in the same way for He lines, taking He I and He II lines separately. Finally we define for model i:

$$\chi_i^2 = \chi_i^2(\text{H}) + \chi_i^2(\text{He I}) + \chi_i^2(\text{He II})$$

so that the best fit is adopted to be that of the model with the minimum value of χ_i^2 .

We have carried on the exercise for a model with $T_{\text{eff}}=40\,000 \text{ K}$, $\log g=3.40$, $\epsilon=0.10$ and $\xi=15 \text{ kms}^{-1}$ as the *observed* spectrum. In Fig. 4 we have plotted contour levels of χ^2 in the $T_{\text{eff}} - \log g$ plane for $\epsilon = 0.10$. We see that, at this He abundance, there are two models that fit well the *observation*, with parameters $T_{\text{eff}}=40\,000 \text{ K}$, $\log g=3.40$ and $T_{\text{eff}}=42\,000 \text{ K}$, $\log g=3.45$. Although the last model has a slightly lower value of χ_i^2 (5.190), the

Table 2. χ_i^2 of models of the grid that best fit the *observed* spectrum, with parameters $T_{\text{eff}}=40\,000 \text{ K}$, $\log g=3.40$, $\epsilon=0.10$ and $\xi=15 \text{ kms}^{-1}$, see text for details.

T_{eff}	$\log g$	ϵ	$\chi_i^2(\text{H})$	$\chi_i^2(\text{He I})$	$\chi_i^2(\text{He II})$	χ_i^2
41 000	3.50	0.06	9.46	2.50	9.12	21.07
41 000	3.45	0.08	1.51	2.25	1.09	4.85
40 000	3.40	0.10	1.36	1.40	2.67	5.44
42 000	3.45	0.10	1.00	3.19	1.00	5.19
39 000	3.35	0.12	2.07	1.82	2.06	5.96
40 000	3.35	0.14	6.81	1.60	7.13	15.54

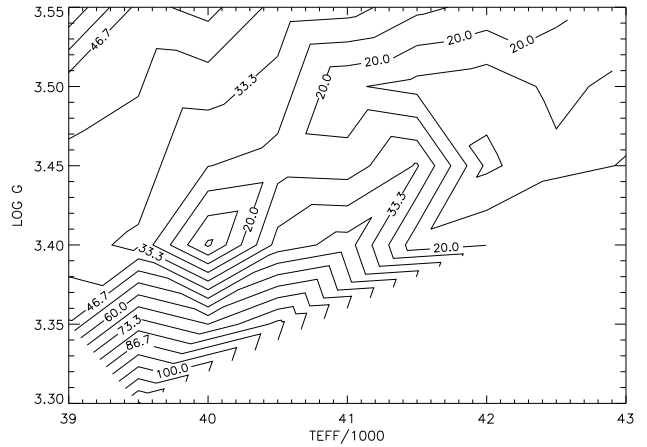


Fig. 4. χ^2 -Contour levels in the $T_{\text{eff}} - \log g$ plane for $\epsilon=0.10$, showing that the best fit for the *observed* model at this abundance is still a model with the same parameters

dispersion in the individual χ_i^2 values is larger, reflecting the fact that looking at the line fits we would choose the other as the best compromise. This is an indication of the differences between both criteria, we should improve our χ^2 fitting criterion in order to match the fitting by eye.

In Table 2 we list the results for the best fits at other He abundances. We see immediately that for $\epsilon = 0.06$ and 0.14 we find large values of χ^2 , indicating a relatively poor fit. On the contrary, the models for $\epsilon=0.12, 0.10, 0.08$ fit with approximately the same quality (without a more detailed study we cannot say whether the difference in χ^2 is significant). In a fit by eye we would choose the model at $\epsilon=0.08$ as the best fit. Actually, this is the model with the lowest value of χ^2 and has a *lower* He abundance than the *observed* spectrum. The reason is that the larger gravity rather than the He abundance mimics the microturbulence effect. In principle, it would be also possible to choose the model with $\epsilon=0.12$, in which the higher He abundance corresponds with a lower gravity. Fig. 5 shows the fit of the “best model” to the *observed* spectrum. The lack of rotation and instrumental broadening makes the differences in He I lines appear evident.

Thus, the conclusion of our exercise is that neglecting microturbulence will change slightly the derived stellar

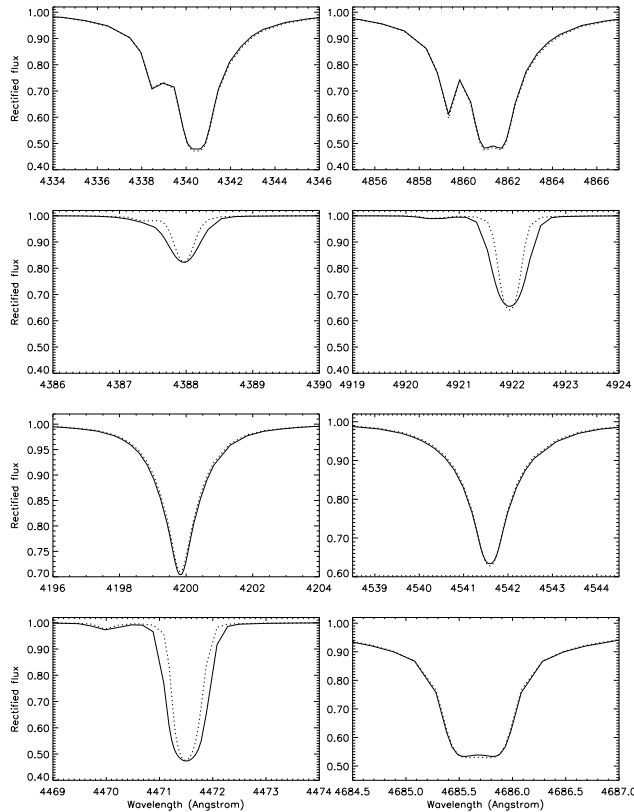


Fig. 5. The fit of the “best model” (dotted, $T_{\text{eff}} = 41\,000$ $\log g = 3.45$ $\epsilon = 0.08$, $\xi = 0$ km s^{-1}) to the *observed* one (solid, $T_{\text{eff}} = 40\,000$ $\log g = 3.40$ $\epsilon = 0.10$, $\xi = 15$ km s^{-1}).

parameters, but keeping them within our standard error box (see next Sect.). The direction in which parameters are moved will depend on the criteria used for defining a model as “the best model fit”, such as the relative weight given to different lines, or to the core and wings of a line. Thus the definition of these criteria for the “best model” will be a critical point of any future automatic fitting procedure, which will soon be demanded by new observing capabilities.

4. Spectral analysis including microturbulence

Now we want to see the difference we obtain in the derived parameters of real observed O stars spectra when we include microturbulence in the calculations. We selected two late-O supergiants to see how our results match with previous works, as well as one intermediate and two early ones, in order to cover the whole O spectral type. We chose HD 5 689 in particular, an O6 V fast rotator with a high He-overabundance derived in previous works without microturbulence (see Herrero et al., 2000), to check how it can modify this strong overabundance.

The description of the observations and data reduction can be found in Herrero et al. (1992, 2000).

To analyse stellar spectra we first determine the projected rotational velocity of the star (see Herrero et al. 1992 for details). This is an additional parameter that, in fact, reduces the effect of microturbulence in the derivation of stellar parameters. The results of the analyses are listed in Table 3.

The fitting procedure and adopted errors of ± 1500 K in T_{eff} , ± 0.1 in $\log g$ and ± 0.03 in ϵ are explained in Herrero et al. (1999).

To make the new analyses with microturbulence we construct a model with the same parameters but for $\xi = 15$ km s^{-1} , and also a small grid around it with changes in T_{eff} of ± 500 to 2000 K, in $\log g$ of ± 0.05 to 0.15 dex and in ϵ of ± 0.02 to 0.04. These small changes are suggested by the results of the preceding section, and are in fact confirmed by the small differences in the fit we see between the two models at 0 and 15 km s^{-1} . The new best fit is found as explained above, and it gives the new parameters for the star at $\xi = 15$ km s^{-1} .

All the stars except HDE 338 926 have been previously analyzed by our group without microturbulence (Herrero et al., 1992, 2000). In the present analysis, small differences for the stars in common, specially with respect to the first reference, can be found due to the larger weight given here to He I $\lambda 4387$, rather than to He I $\lambda 4922$, and to the inclusion of line-blocking in the calculations (the temperatures of the late type supergiants are slightly hotter in the present analysis). All this also helps to solve the small difference between He I $\lambda 4387$ and He I $\lambda 4922$ found in Herrero et al. (1992) for these late O supergiants.

In Table 3 we see the results for the five stars. Changes in the parameters induced by microturbulence are not beyond the standard error box of the analysis, and in particular, we see that He abundance is reduced for four of the stars, but only slightly. In Table 4 we see the values obtained for the radius, mass and luminosity, following the same procedures outlined in Herrero et al. (1992). We see that changes are not significant. (We point out that the values for mass, radius and luminosity given in Table 4 for HD 210 809 and HD 18 409 differ slightly from those given in Herrero et al. (1992). These differences are not due to the new parameters, but to a change in the distance module. Herrero et al. used the values from Humphreys (1978), while we use the values from Garmany & Stencel (1992)).

In Figs. 6 to 10 we can see the fits with microturbulence 0 and 15 km s^{-1} . The quality of the fits to individual lines is the same at both values, although the triplet line He I $\lambda 4471$ becomes stronger at 15 km s^{-1} , which produces an improved fit, but not to the extent as to completely resolve the so-called dilution effect. Sometimes, a compromise between He I $\lambda 4387$ and He I $\lambda 4922$ is adopted, like in HD 5 689 and HD 210 809 (realize that for 15 km s^{-1} the first one is slightly weak and the second one slightly strong).

With respect to HDE 338 926, that has been analyzed here for the first time, we have to point out that the anal-

Table 3. Stellar parameters with values of microturbulence of 0 and 15 kms^{-1} . Effective temperatures are given in K and surface gravities in c.g.s. units. Spectral classifications are taken from Walborn (1973), except that of HD 5689, which is taken from Garmany & Vacca (1991), and that of HDE 338926, which is taken from Humphreys (1978; Humphreys lists this star as BD+24 3866). Some final parameters are extrapolated as we could not converge the model with the indicated values of $\log g$ but others with $\log g$ 0.05 larger, with all other parameters the same. This is indicated by giving the parameters in italics

Star	Clasif.	$V_r \sin i$ kms^{-1}	T_{eff}		$\log g$		ϵ	
			0 kms^{-1}	15 kms^{-1}	0 kms^{-1}	15 kms^{-1}	0 kms^{-1}	15 kms^{-1}
HD 14947	O5 If ⁺	140	45 000	<i>45 000</i>	3.50	<i>3.45</i>	0.15	<i>0.15</i>
HD 5689	O6 V	250	40 000	40 000	3.40	3.35	0.25	0.22
HDE 338926	O8 f	130	<i>34 000</i>	<i>34 500</i>	<i>3.00</i>	<i>3.00</i>	<i>0.15</i>	<i>0.13</i>
HD 210809	O9 Iab	120	33 500	34 500	3.10	3.15	0.10	0.08
HD 18409	O9.7 Ib	160	31 500	32 000	3.10	3.10	0.11	0.09

Table 4. Radius, mass and luminosity for the analyzed objects. As in Table 3, italic numbers mean values obtained by extrapolation

Star	R/R_{\odot}		M/M_{\odot}		$\log(L/L_{\odot})$	
	0 kms^{-1}	15 kms^{-1}	0 kms^{-1}	15 kms^{-1}	0 kms^{-1}	15 kms^{-1}
HD 14947	14.8	<i>14.9</i>	26.5	<i>24.1</i>	5.91	<i>5.91</i>
HD 5689	7.7	7.8	7.8	7.4	5.13	5.14
HDE 338926	<i>24.4</i>	<i>24.3</i>	<i>23.8</i>	<i>23.5</i>	<i>5.86</i>	<i>5.88</i>
HD 210809	18.2	17.9	16.0	17.4	5.57	5.61
HD 18409	18.8	18.8	18.7	18.6	5.50	5.52

ysis has been very difficult. The final parameters are extrapolated beyond the models we could converge. However, we are confident that these parameters do characterize the star appropriately (or as appropriately as those of other stars), because the fits with already converged models are reasonably good, and because we are able to fit the star with converged models when we do not consider line-blocking. Thus, it is only the small temperature increase introduced by line-blocking that moves the star beyond the convergence region. The value we obtain for the evolutionary mass, derived from the tracks by Schaller et al., (1992), is $57.6 M_{\odot}$ without microturbulence, and $56.8 M_{\odot}$ with 15 kms^{-1} . Comparing with the values in Table 4, it is clear that HDE 338926 also shows a mass discrepancy, as usual. Of course, we will have to reanalyze HDE 338926 in the future with spherical, mass lossing models.

5. Discussion

We will not go here into the discussion of the real physical entity of microturbulence, neither on the validity of the approximation of small scale turbulent movements assumed to introduce it just as an extra Doppler width, which may be not suitable for the big values we deal with. This is beyond the scope of this work. As explained in Sect. 2 we do not introduce microturbulence in the structure calculations because we think that, having neglected other motions, it is actually not more physically consistent to introduce a turbulent pressure term. We just accept the necessity of using microturbulence in the analysis of stel-

lar spectra, specially in the determination of metal abundances, that is our final interest.

We find that contrary to our previous considerations, He I lines and He II λ 4686 do have profiles sensitive to the usual values of microturbulence found in OB stars. We confirm this for the whole range of parameters describing O and early B spectra, in agreement with McErlean et al. (1998) and Smith & Howarth (1998) for early B and late O supergiants respectively. This sensitivity is first due to the fact that the Stark broadening is not dominating completely these profiles and second to the high values of microturbulence involved, that are comparable to the thermal velocity of He ions. Taking $(0.84 T_{\text{eff}})$ as representative of the temperature in the zone of formation of the lines, we find that for $T_{\text{eff}} = 30\,000 \text{ K}$ v_{th} of He ions is 10 kms^{-1} , and for $T_{\text{eff}} = 45\,000 \text{ K}$ it is 12 kms^{-1} . For H ions, with a fourth of the He atomic weight, thermal velocities are two times larger, so thermal broadening and Stark broadening dominate the profile. For all other He II lines Stark broadening is hiding the effect of microturbulence.

Quantifying the effect of microturbulence on the determination of stellar parameters we find that they are not changed beyond the standard error box of our analyses. This implies that for stars with high He overabundances, such as HD 5689 analysed here, the *He discrepancy* will not be solved by considering microturbulence. This result is also supported by what we obtained in Sect. 3.

This seems to be in contradiction with Smith & Howarth (1998) and McErlean et al. (1998), who affirm

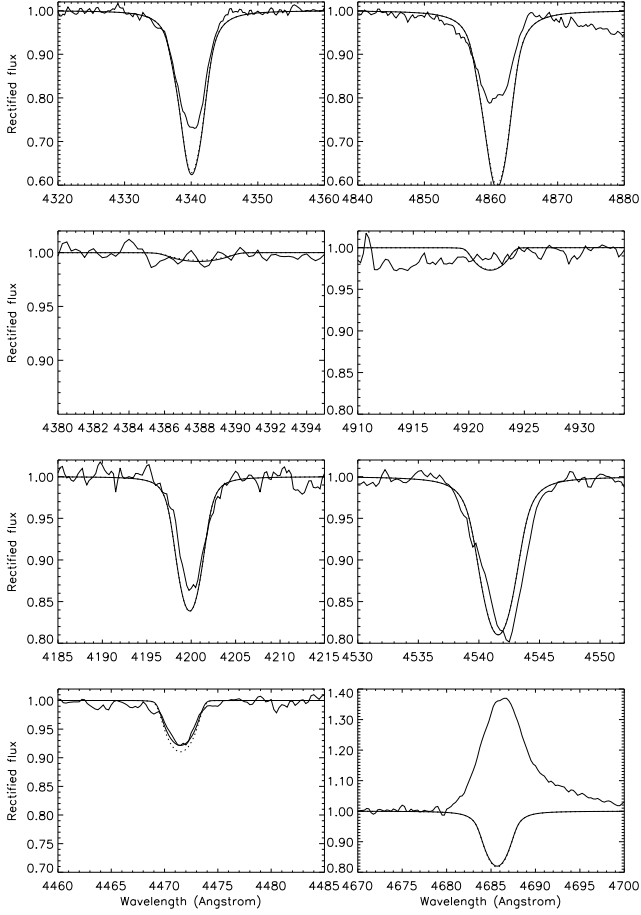


Fig. 6. Fits with $\xi = 0 \text{ km s}^{-1}$ (solid line) and $\xi = 15 \text{ km s}^{-1}$ (dotted) to the star HD 14947. The parameters are $T_{\text{eff}} = 45000$, $\log g = 3.50$, $\epsilon = 0.15$ at $\xi = 0 \text{ km s}^{-1}$ and the same at 15 km s^{-1} , which are the converged models closest to the final adopted parameters, with $\log g = 3.45$

that solar He abundances are found for the supergiants they analyse, when microturbulence is considered. However, the situation is still unclear, as an analysis of published results can show.

Let us begin with the He overabundances obtained by Herrero et al. (1992). Following the argument by Smith & Howarth (1998) and McErlean et al. (1998), the preferred use of the strong line He I λ 4922 in the analyses (slightly more sensitive to microturbulence than He I λ 4387) would be responsible for the high He abundances found in that work. As a conclusion, the derived He overabundances would be an artifact introduced by the neglect of microturbulence.

This argument applies in the cases in which Herrero et al. (1992) found a discrepancy between He I λ 4922 and He I λ 4387, but not in the rest of the cases.

In Fig. 11 we have plotted He abundance versus T_{eff} , as derived by Herrero et al. (1992), using different symbols for stars for which a discrepancy between these two lines was reported. We can see that the priority given to He I λ

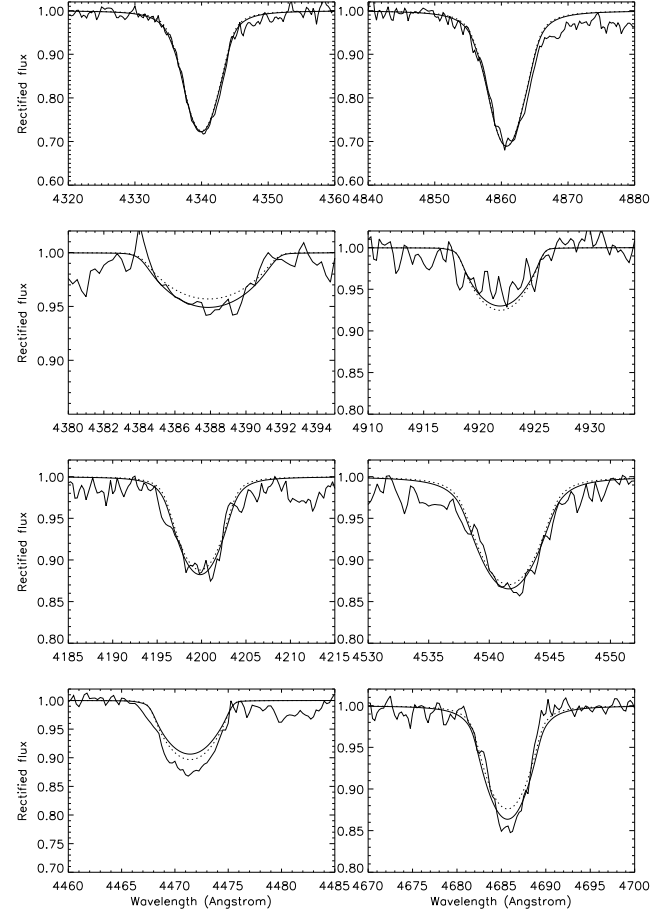


Fig. 7. Fits with $\xi = 0 \text{ km s}^{-1}$ (solid line) and $\xi = 15 \text{ km s}^{-1}$ (dotted) to the star HD 5689. The parameters are $T_{\text{eff}} = 40000$, $\log g = 3.40$, $\epsilon = 0.25$ at $\xi = 0 \text{ km s}^{-1}$ and $T_{\text{eff}} = 40000$, $\log g = 3.35$, $\epsilon = 0.22$ at $\xi = 15 \text{ km s}^{-1}$

4922 can affect some of the abundances derived, specially at lower temperatures.

To illustrate the situation, let us briefly discuss one of these objects for which Herrero et al. report a difference between He I λ 4922 and He I λ 4387: HD 210809. This star has been analyzed here again, where we have given more weight to He I λ 4387 (contrary to Herrero et al.). The final difference between the He abundance obtained here with a microturbulence of 15 km s^{-1} and that obtained by Herrero et al. is 0.04 (our new He abundance being lower). This, however, has to be ascribed to different effects. First, giving more weight to He I λ 4387 in absence of microturbulence results in a higher temperature (as already stated by Herrero et al.), which leads to a lower He abundance to keep the fit of He II lines. The effect of line blocking, not included in Herrero et al., goes in the same direction. This accounts for a difference of 0.02 and the additional difference of 0.02 is purely due to microturbulence (see Table 3). Comparing our Fig. 9 with Fig. 5 of Herrero et al. (1992) we see that the effects con-

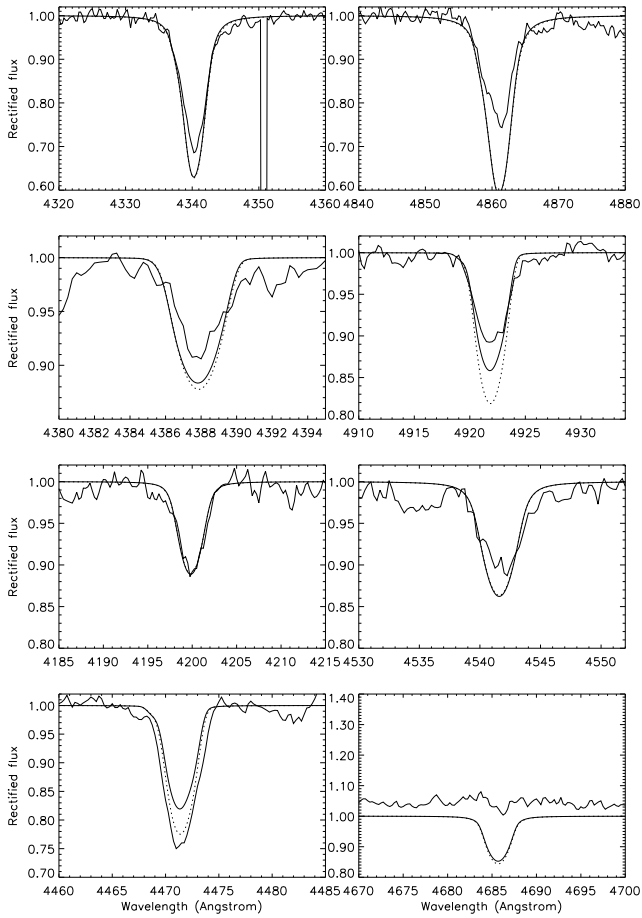


Fig. 8. Fits with $\xi = 0 \text{ km s}^{-1}$ (solid line) and $\xi = 15 \text{ km s}^{-1}$ (dotted) to the star HD 338 926. The parameters are $T_{\text{eff}}=34000$, $\log g=3.05$, $\epsilon=0.15$ at $\xi = 0 \text{ km s}^{-1}$ and $T_{\text{eff}}=34500$, $\log g=3.10$, $\epsilon=0.13$ at $\xi = 15 \text{ km s}^{-1}$. Again these are the closest models that could be converged, for a final adopted $\log g$ of 3.00

considered here help to reduce the discrepancy between the two He I lines.

The discrepancy between He I λ 4387 and He I λ 4922 found by Herrero et al. (1992) is larger at lower temperatures, and thus, around 30 000 K it cannot be solved by varying T_{eff} or introducing line blocking. Therefore, around or below this temperature microturbulence is at present the only considered effect that could bring them into agreement.

In the literature we can find analyses of early B and late O supergiants including microturbulence (Gies & Lambert, 1992, Smith & Howarth, 1994, 1998, Smith et al., 1998, McErlean et al., 1998). In Table 5 we list stars for which parameters have been derived with and without microturbulence.

Comparisons in Table 5 have to be done with care. It mixes results from different authors and different criteria. We see however that it indicates that the changes found here are consistent with those of other authors, i.e.,

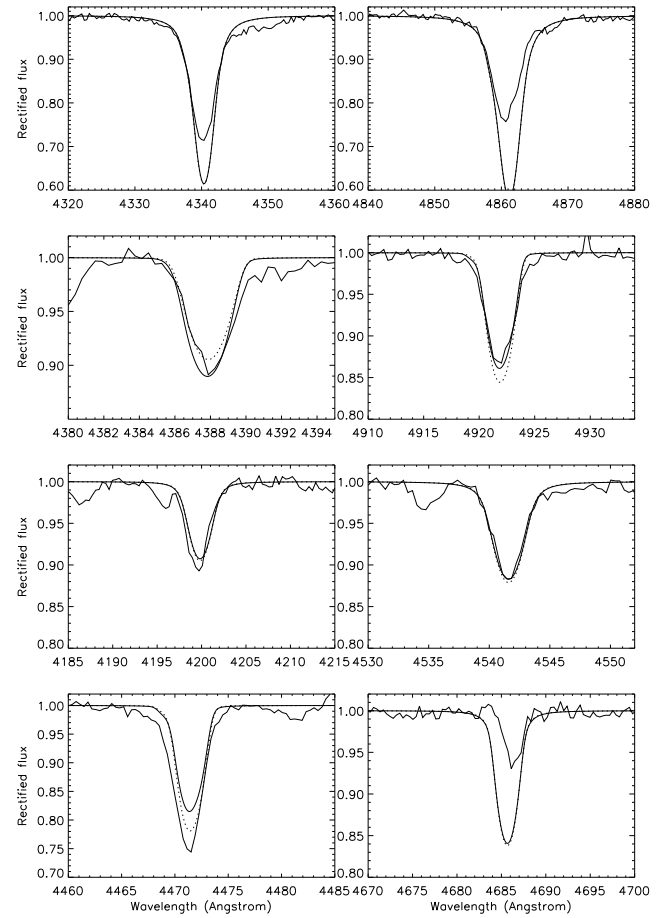


Fig. 9. Fits with $\xi = 0 \text{ km s}^{-1}$ (solid line) and $\xi = 15 \text{ km s}^{-1}$ (dotted) to the star HD 210 809. The parameters are $T_{\text{eff}}=33500$, $\log g=3.10$, $\epsilon=0.10$ at $\xi = 0 \text{ km s}^{-1}$ and $T_{\text{eff}}=34500$, $\log g=3.15$, $\epsilon=0.08$ at $\xi = 15 \text{ km s}^{-1}$

stellar parameters are changed within the uncertainties adopted here. These changes do not follow a clear, systematic pattern (i.e., going always in the same direction when introducing microturbulence) and thus we conclude that the effect of microturbulence is indeed not larger than present-day uncertainties. An exception to this might be κ Ori, which shows a large change in He abundance. However, this large reduction of the He abundance found by McErlean et al. (1998) as compared to Lennon et al. (1991) is accompanied by a large change in the stellar parameters. Even if we attribute the whole change to the effect of microturbulence (and not to a new analysis with new data and more refined calculations) we see that κ Ori is by far the coolest of the stars in Tables 3 and 5 and thus we expect a larger influence of microturbulence for it. In addition, we note that McErlean et al. (1998) do not exclude a larger He abundance for this star. We conclude that data in the literature do not lead to the conclusion that the He discrepancy in O and early B supergiants is completely due to microturbulence, although microturbulence helps to reduce it.

Table 5. OB supergiants with parameters determined with and without microturbulence. Values of microturbulence vary between 10 and 15 kms^{-1} . References are as follows: (1) Herrero et al. (2000); (2) this work; (3) Herrero et al. (1992); (4) Smith & Howarth (1994); (5) Smith et al. (1998); (6) Smith & Howarth (1998); (7) Lennon et al. (1991); (8) McErlean et al. (1998)

Star	Clasif.	$V_r \sin i$ kms^{-1}	T_{eff}		$\log g$		ϵ		Ref.	
			$\xi = 0$	$\xi \neq 0$	$\xi = 0$	$\xi \neq 0$	$\xi = 0$	$\xi \neq 0$	$\xi = 0$	$\xi \neq 0$
HD 14 947	O5 If ⁺	140	45.0	45.0	3.50	3.45	0.15	0.15	1	2
HD 5 689	O6 V	250	40.0	40.0	3.40	3.35	0.25	0.22	1	2
HD 210 809	O9 Iab	100	33.0	34.5	3.10	3.15	0.12	0.08	3	2
HD 154 368	O9.5 Iab	85	33.0	32.0	3.07	3.00	0.13	0.13	4	5
HD 123 008	ON9.5 Iab	90	33.5	33.0	3.07	3.05	0.17	0.15	4	5
HD 152 003	O9.7 Iab	80	30.8	29.7	2.90	3.10	0.09	0.09	6	6
				30.5		3.00		0.09		5
HD 18 409	O9.7 Ib	160	31.0	32.0	3.10	3.10	0.12	0.09	3	2
HD 154 811	OC9.7 Iab	125	31.5	31.0	3.15	3.10	0.09	0.09	4	5
κ Ori	B0.5 Ia	80	25.0	27.5	2.70	3.00	0.20	0.10	7	8

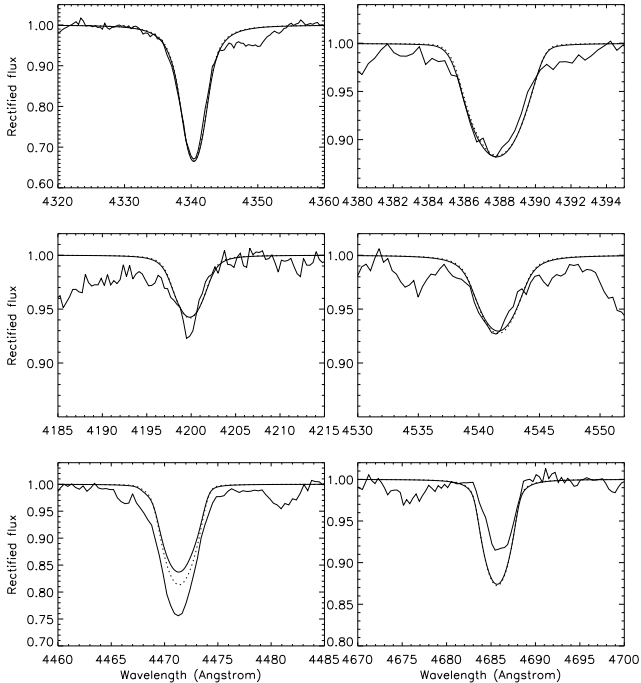


Fig. 10. Fits with $\xi = 0 \text{ kms}^{-1}$ (solid line) and $\xi = 15 \text{ kms}^{-1}$ (dotted) to the star HD18409. The parameters are $T_{\text{eff}} = 31\,500$, $\log g = 3.10$, $\epsilon = 0.11$ at $\xi = 0 \text{ kms}^{-1}$ and $T_{\text{eff}} = 32\,000$, $\log g = 3.10$, $\epsilon = 0.09$ at $\xi = 15 \text{ kms}^{-1}$. We could not use neither H_β nor $\text{He I } \lambda 4922$ for the fit, as we don't have observations of this star in this range.

Except for the discussed reduction of the He abundance, we do not see a clear pattern in the parameter changes in Tables 3 and 5. T_{eff} and $\log g$ can both increase or decrease when microturbulence is introduced, and thus we are tempted to conclude that these changes are still dominated by internal inconsistencies in the analyses that appear when we compare values that cannot be distinguished within the adopted uncertainties.

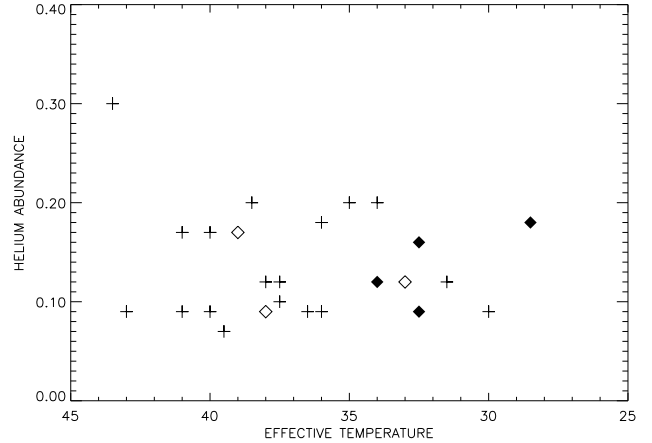


Fig. 11. ϵ versus T_{eff} (in thousands of Kelvin) in the sample of Herrero et al. (1992). Filled diamonds represent stars for which Herrero et al. report a large discrepancy between $\text{He I } \lambda 4922$ and $\text{He I } \lambda 4387$. Open diamonds represent stars for which Herrero et al. report a moderate discrepancy between these two lines. Plus signs represent stars for which Herrero et al. do not report a discrepancy

About the problem of the consistency of the fits to He I lines, we find that the dilution of $\text{He I } \lambda 4471$ is only partially solved, even when line-blocking is considered as here. The fits to the rest of He I lines do not improve much either in the stars we analyze here. So the consideration of both microturbulence and line-blocking in the analysis cannot completely make an agreement between the results from triplet and singlet He I lines, though they help to improve it.

6. Conclusions

We study for the first time the effect of microturbulence in the whole O spectral range, from late to early O types.

Introducing microturbulence in the solution of the statistical equilibrium and transfer equations, and then in the formal solution (i.e., in the absorption coefficient), we conclude that for higher gravities the effect in the lines is negligible. This together with the low values of microturbulence usually found for high luminosity class stars, lead us to conclude that only O supergiants have sensitivity to microturbulence effects at a given T_{eff} .

In examining the behaviour with microturbulence of the lines we use in our analysis, we show that only He I lines and the core of He II λ 4686 Å are sensitive to microturbulence. For He I lines we show that, as should be expected, there is not a constant pattern for each line, but it depends on the parameters considered, that determine the strength of the line and its degree of saturation. This invalidates generalizations to the whole O spectral range made upon results obtained just for a certain spectral type.

In order to quantify the sensitivity of stellar parameters to microturbulence we find that changes in the parameters induced by a value of microturbulence of 15 km s^{-1} are enclosed within the standard error box of our analyses. We think that the lack of a clear pattern in the changes induced in T_{eff} and $\log g$ is just due to the fact that we are varying the parameters within this error box. We do however find a systematic change in ϵ towards lower He abundances when microturbulence is introduced. In particular we find that late O supergiants show a decrease of 0.02–0.04 in ϵ (this last value when including other effects that add to microturbulence), which is in agreement with previous results pointing to the inverse relation between the microturbulence assumed and the He abundance obtained (Smith & Howarth 1998). Early types are less sensitive to microturbulence, and might not show a difference in the derived He abundance.

Thus microturbulence is not capable of explaining the *He discrepancy* at all for early O stars, and neither it is for late O types with high overabundances.

Looking to individual lines we find that the fits to He I λ 4471 Å are improved when considering microturbulence, but not to the extent of completely explaining its dilution. On the other hand He I $\lambda\lambda$ 4922, 4387 Å are sometimes slightly better and sometimes slightly worse fitted, in the last case with model cores a bit too strong or a bit too weak, respectively. The rest of the lines keep the same quality in the fit. The He I *lines problem* is therefore only partially solved by simply considering microturbulence, even with line-blocking included in the model profiles.

Therefore our conclusion is that microturbulence is affecting the derivation of stellar parameters, but its effect is comparable to the adopted uncertainties. Thus it can reduce moderate He overabundances and solve line fit quality differences, but it cannot explain by itself large He overabundances in O stars, and we are forced to conclude that these are due to other effects, whether real or caused

by artifacts in our analyses. This last point will probably not find a definitive answer until we are able to derive reliable abundances of C, N and O in the atmospheres of O stars that we can correlate with the He abundances.

Acknowledgements. We want to thank Neil McErlean and Danny Lennon for their help, suggestions and many clarifying discussions. AH wants to acknowledge support for this work by the spanish DGES under project PB97-1438-C02-01

References

- Becker S.R., Butler K., 1989, A&A 209, 244
 Butler, K., Giddings, J., 1985, in Newsletter on Analysis of Astronomical Spectra, Volume 9, Daresbury Laboratory
 Dennisenkov P.A., 1994, A&A 287, 113
 Garmany C.D., Stencel R.E., 1992, A&ASS 94, 211
 Garmany C.D., Vacca W.D., 1991, PASP 103, 347
 Gies D.R., Lambert D.L., 1992, ApJ 387,673
 Hardorp J., Scholz M., 1970, ApJS 19,193
 Heger A., 1998, PhD Thesis, Technische Universität München
 Herrero A., 1994, Space Sci. Rev. 66, 137
 Herrero A., Kudritzki R.P., Vilchez J.M. et al., 1992, A&A 261,209
 Herrero A., Kudritzki R.P., Gabler R., Vilchez J.M., Gabler A., 1995, A&A 297, 556
 Herrero A., Corral L.J., Villamariz M.R., Martín E.L., 1999, A&A 348, 542
 Herrero A., Puls J., Villamariz M.R., 2000, A&A 354, 193
 Hubeny I., Heap S.R., Altner B., 1991, ApJL 377,L33
 Humphreys R.M., 1978, ApJS 38, 309
 Israelian G., Herrero A., Musaev F. et al., 2000, MNRAS, in press
 Kilian J., Becker S.R., Gehren T., Nissen P.E., 1991, A&A 244, 419
 Kudritzki R.P., 1992, A&A 266,395
 Kunze D., 1995, Ph. D. Thesis, Ludwig-Maximillian University Munich
 Lamers H.J.G.L.M., 1972, A&A 17, 34
 Lamers H.J.G.L.M., Achmad L., 1994, A&A 291, 856
 Langer N., 1992, A&A 265, L17
 Langer N., Heger A., 1998, A&A 334, 210
 Lennon D.J., Dufton P.L., 1986, A&A 155, 79
 Lennon D.J., Kudritzki R.P., Becker, S.R. et al., 1991, A&A 252, 498
 Maeder A., Zahn J.-P., 1998, A&A 334, 1000
 Maeder A., Meynet G., 2000, ARA&A, in press
 McErlean N.D., Lennon D.J., Dufton, P.L., 1998, A&A 329, 613
 Meynet G., Maeder A., 1997, A&A 321, 465
 Schaller G., Schaerer D., Meynet G., Maeder A., 1992, A&AS 96, 269
 Smartt S.J., Dufton P.L., Lennon D.J., 1997, A&A 326, 763
 Smith K.C., Howarth I.D., 1994, A&A 290,868
 Smith K.C., Howarth I.D., 1998, MNRAS 299,1146
 Smith K.C., Howarth I.D., Siebert K., 1998, Proc. of Boulder–Munich II: Properties of Hot, Luminous Stars, ed. I.D. Howarth, ASP Conf. Series V. 131, p. 153
 Vrancken M., 1997, Ph. D. Thesis, Vrije Universiteit Brussel
 Voels S.A., Bohannan, B., Abbott, D.C., Hummer, D.G., 1989, ApJ 340, 1073
 Walborn N.R., 1973, AJ 78, 1067